Biochemical and Biophysical Research Communications 435 (2013) 300–305

Contents lists available at SciVerse ScienceDirect

Biochemical and Biophysical Research Communications

journal homepage: www.elsevier.com/locate/ybbrc

Stabilisation of Na,K-ATPase structure by the cardiotonic steroid ouabain

Andrew J. Miles [a], Natalya U. Fedosova [b], Søren V. Hoffmann [c], B.A. Wallace [a], Mikael Esmann [b,*]

[a] Institute of Structural and Molecular Biology, Birkbeck College, University of London, London WC1E 7HX, UK
[b] Department of Biomedicine, Aarhus University, DK-8000 Aarhus, Denmark
[c] ISA, Department of Physics and Astronomy, Aarhus University, DK-8000 Aarhus, Denmark

ARTICLE INFO

Article history:
Received 9 April 2013
Available online 22 April 2013

Keywords:
Synchrotron radiation circular dichroism (SRCD) spectroscopy
Na,K-ATPase
Ouabain
Membrane protein
Thermal melt curves
Enzyme activity

ABSTRACT

Cardiotonic steroids such as ouabain bind with high affinity to the membrane-bound cation-transporting P-type Na,K-ATPase, leading to complete inhibition of the enzyme. Using synchrotron radiation circular dichroism spectroscopy we show that the enzyme-ouabain complex is less susceptible to thermal denaturation (unfolding) than the ouabain-free enzyme, and this protection is observed with Na,K-ATPase purified from pig kidney as well as from shark rectal glands. It is also shown that detergent-solubilised preparations of Na,K-ATPase are stabilised by ouabain, which could account for the successful crystallisation of Na,K-ATPase in the ouabain-bound form. The secondary structure is not significantly affected by the binding of ouabain. Ouabain appears however, to induce a reorganization of the tertiary structure towards a more compact protein structure which is less prone to unfolding; recent crystal structures of the two enzymes are consistent with this interpretation. These circular dichroism spectroscopic studies in solution therefore provide complementary information to that provided by crystallography.

© 2014 Published by Elsevier Inc.

1. Introduction

The cardiotonic steroid ouabain is an extremely potent and specific inhibitor of Na,K-ATPase, the enzyme system responsible for active transport of Na^+ and K^+ across the plasma membrane of most cells [1]. In addition to the inhibition of Na,K-ATPase, which is the basis for the positive inotropic effect of digitalis glycosides leading to strengthening of heart muscle important in congestive heart failure, these compounds have been implicated in cellular signaling [2]. The properties of the ouabain-bound form of Na,K-ATPase is therefore currently of considerable interest.

Crystal structures of pig and shark Na,K-ATPase in both the absence [3,4] and presence of ouabain [5,6] have been determined. There is a strong similarity between the structures of the shark and pig α-subunits, and ouabain-induced re-arrangements can be seen for the enzymes from both species.

We have previously analysed the thermal stabilities of the ouabain-free enzymes using synchrotron radiation circular dichroism (SRCD) spectroscopy [7], revealing the structural changes associated with the enzyme inactivation. Here we address the effect of ouabain on their thermal stability, comparing structure in the membranes as well as in three detergent-solubilised states (using the nonionic detergent octaethyleneglycoldodecylmonoether ($C_{12}E_8$)). Furthermore, the properties of the $C_{12}E_8$-solubilised enzymes are interesting since $C_{12}E_8$-solubilisation [8] is the first step in crystallisation procedures.

We show that Na,K-ATPase-ouabain complexes of the shark and pig enzymes are more structurally stable towards thermal denaturation than the ouabain-free forms. The secondary structures are not changed by ouabain binding, and the thermal stability conferred by ouabain is therefore most likely attributable to a reorganization of the tertiary structure. Ouabain has also a stabilising effect on the solubilised enzymes at low detergent/protein ratios, where the native structure is fully preserved.

2. Material and methods

2.1. Protein purification and activity measurements

Na,K-ATPase from the salt gland of *Squalus acanthias* was prepared according to the method of Skou and Esmann [9], omitting the saponin treatment. Na,K-ATPase from pig kidney microsomal membranes was prepared by treatment with SDS and purified by differential centrifugation [10]. The specific activities of both

Abbreviations: $C_{12}E_8$, octaethyleneglycoldodecylmonoether; DSC, differential scanning calorimetry; DSSP, database of secondary structure assignments; HT, high tension; SRCD, synchrotron radiation circular dichroism; SVD, single value deconvolution; T_m, midpoint temperature; α-subunit, the 112 kD catalytic subunit bearing the ligand binding sites; αM1, the first N-terminal transmembrane segment of the α-subunit.

* Corresponding author. Address: Department of Biomedicine, Ole Worms Allé 6, Aarhus University, DK-8000 Aarhus, Denmark. Fax: +45 8612 9599.
E-mail address: me@biophys.au.dk (M. Esmann).

0006-291X/$ - see front matter © 2014 Published by Elsevier Inc.
http://dx.doi.org/10.1016/j.bbrc.2013.04.021

enzyme preparations were approximately 30 μmol ATP hydrolysed/mg protein per min at 37 °C [11]. The purified membrane preparations were filtered through a 8 μm Millipore filter (SCWP) and stored at −20 °C in a buffer containing 20 mM $Tris_2SO_4$, 4 mM $MgSO_4$, 3 mM Na_2HPO_4, 25% glycerol and 0 or 0.1 mM ouabain (pH 7.4).

The temperature stability of Na,K-ATPase enzyme activity in the absence of ouabain was determined for pig and shark enzymes in the membrane-bound form as well as in the detergent-solubilised state as previously described [7,12].

2.2. Sample preparation for SRCD spectroscopic measurements

Purified frozen preparations (at a protein concentration of approximately 8 mg/ml) in 20 mM $Tris_2SO_4$, 4 mM $MgSO_4$, 3 mM Na_2HPO_4, 25% glycerol (pH 7.4) with 0 or 0.1 mM ouabain were thawed and diluted to approximately 4 mg/ml with 20 mM $Tris_2SO_4$, 4 mM $MgSO_4$, 3 mM Na_2HPO_4, 25% glycerol (pH 7.4) with 0 or 0.1 mM ouabain. $C_{12}E_8$-solubilised samples were prepared as follows: the purified frozen preparations were thawed and diluted with a $C_{12}E_8$-solution in 20 mM $Tris_2SO_4$, 4 mM $MgSO_4$, 3 mM Na_2HPO_4, 25% glycerol (pH 7.4) with 0 or 0.1 mM ouabain to give a final protein concentration of ~4 mg/ml and $C_{12}E_8$/protein ratios of 3.3, 13.3 or 26.3 mg $C_{12}E_8$/mg protein. The addition of detergent was done on ice, and the solubilised enzyme brought to 20 °C. Protein concentration was determined using the Lowry method [13] which had previously been calibrated for Na,K-ATPase by quantitative amino acid analysis [14].

2.3. SRCD spectroscopy

SRCD spectra were collected on beamline CD1 [15,16] at ISA, Centre for Storage Ring Facilities, Aarhus University, Denmark. Protocols for collecting SRCD data are described in Ref. [7]. Briefly, SRCD spectra were collected in a 0.0015 cm pathlength quartz Suprasil cell (Hellma, UK), over the wavelength range 280 nm to 175 nm with a 1 nm step size and an averaging time of 2 s. Spectra were collected over a set temperature range of 20 °C to 85 °C in 5 °C increments allowing 3 min equilibration time at each temperature. The temperature was calibrated using a thermistor placed inside a cell containing water. The temperatures of the scans were then annotated with the actual rather than set temperatures. Three scans measured at each temperature were averaged and subtracted from the averaged three scans of a buffer baseline. The resulting spectra were calibrated against a spectrum of camphorsulfonic acid [17] collected after each beam-fill then converted to units of delta epsilon using mean residue weights of 110.3 and 111.7 for shark and pig proteins, respectively. All processing was carried out using the CDTool software [18]. Thermal denaturation curves were obtained by plotting the CD signal at 194 nm and fitting a Boltzman sigmoidal function. Error bars represent the standard deviation between three repeat measurements. Secondary structure analyses were carried out using the DichroWeb analysis server [19]. Values from the algorithms CONTINLL [20,21], SELCON [22] and CDDSTR [22] (using reference set SMP180 [23]) were averaged and their standard deviations reported. SMP180 is a new reference data set specifically devised for use with membrane proteins. Consequently the calculated values reported here slightly different from the values for the samples reported earlier [7] based on analyses done with data sets derived only from soluble proteins; however all the trends are the same.

SRCD spectra have been deposited in the Protein Circular Dichroism Data Bank (PCDDB) located at <http://pcddb.cryst.bbk.ac.uk> with ID codes CD0003991000 to CD0004006000.

2.4. Comparison of crystal structures

Secondary structures were calculated by the DSSP algorithm [24] using the 2Struc website [25] on pig [PDB ID: 3N23 and PDB ID: 3KDP] and shark [PDB ID: 3A3Y and PDB ID: 2ZXE] enzymes with and without ouabain present, respectively (Table 2).

3. Results and discussion

3.1. Thermal denaturation of Na,K-ATPase

Figs. 1A and B shows representative SRCD spectra of membranous shark and pig Na,K-ATPase in the ouabain-bound and the ouabain-free state at temperatures between 20 and 78 °C.

As was previously found [7], the ouabain-free pig enzyme is more thermally stable than shark enzyme with respect to the extent of unfolding, demonstrating a net decrease of 13% of the helical structure when heated from 20 °C to 78 °C, compared to 17% for shark (Table 1). In the presence of ouabain the trend for both enzymes is the same, a net decrease of 13% of the helical structure of pig when heated from 20 °C to 78 °C compared to 17% for shark (Table 1). The helical content of shark enzyme is slightly larger than for pig at 20 °C (40% vs. 36%) with no significant effect of ouabain on these values (Table 1).

Figs. 1C and D show representative SRCD spectra of solubilised shark and pig Na,K-ATPase at a detergent/protein ratio of 3.3 mg $C_{12}E_8$/mg protein at temperatures 20 °C, 37 °C and 78 °C. At this ratio, the Na,K-ATPases from both species have less helix and more β-sheet than the membrane-embedded samples at 20 °C (Table 1). Pig enzyme is more thermally-stable, showing a decrease in total helical content of 18% between 20 °C and 78 °C, Table 1, which was similar to that observed in previous experiments at the lower ratio of 2.0 mg/mg [7]. For shark enzyme the net amount of helix lost is 19%. For both enzymes, the helix loss in the solubilised state is slightly higher than in membranes (Table 1).

3.2. Spectral analyses of thermal denaturation of membranous Na,K-ATPase

Principal component analyses [18] did not significantly distinguish between the ouabain-bound and ouabain-free membranous enzymes at any one temperature. However, analysis of the entire set of thermal titration curves suggest that the ouabain-bound species are considerably stabilised compared to the ouabain-free species. This is shown in Fig. 2, where the SRCD amplitude at 194 nm is plotted as a function of the incubation temperature. The T_m of the pig sample was found to be 61 °C in the ouabain-free state (Fig. 2, filled squares). The ouabain-bound pig enzyme unfolds to approximately the same extent as the ouabain-free species, but the T_m is higher, 64 °C, when ouabain is bound (Fig. 2, open squares).

There is a similar effect of ouabain on the shark enzyme. T_m of the ouabain-free shark sample was found to be 55 °C (Fig. 2, filled circles). The ouabain-bound shark enzyme unfolds to approximately the same extent but the T_m is significantly higher, 60 °C, when ouabain is bound (Fig. 2, open circles). The protective effect of ouabain can also be inferred (Table 1), as deconvolution at 51 °C shows that for the ouabain-bound shark enzyme there is a slightly larger amount of helical structure than in the absence of ouabain. The decrease in helical content comparing 20 and 51 °C is 6% out of the total 17% change in the absence of ouabain and only 4% out of 17% in the presence of ouabain (comparing data at 20, 51 and 78 °C).

We have previously compared the thermally induced loss of enzymatic activity with the structural changes for Na,K-ATPase in

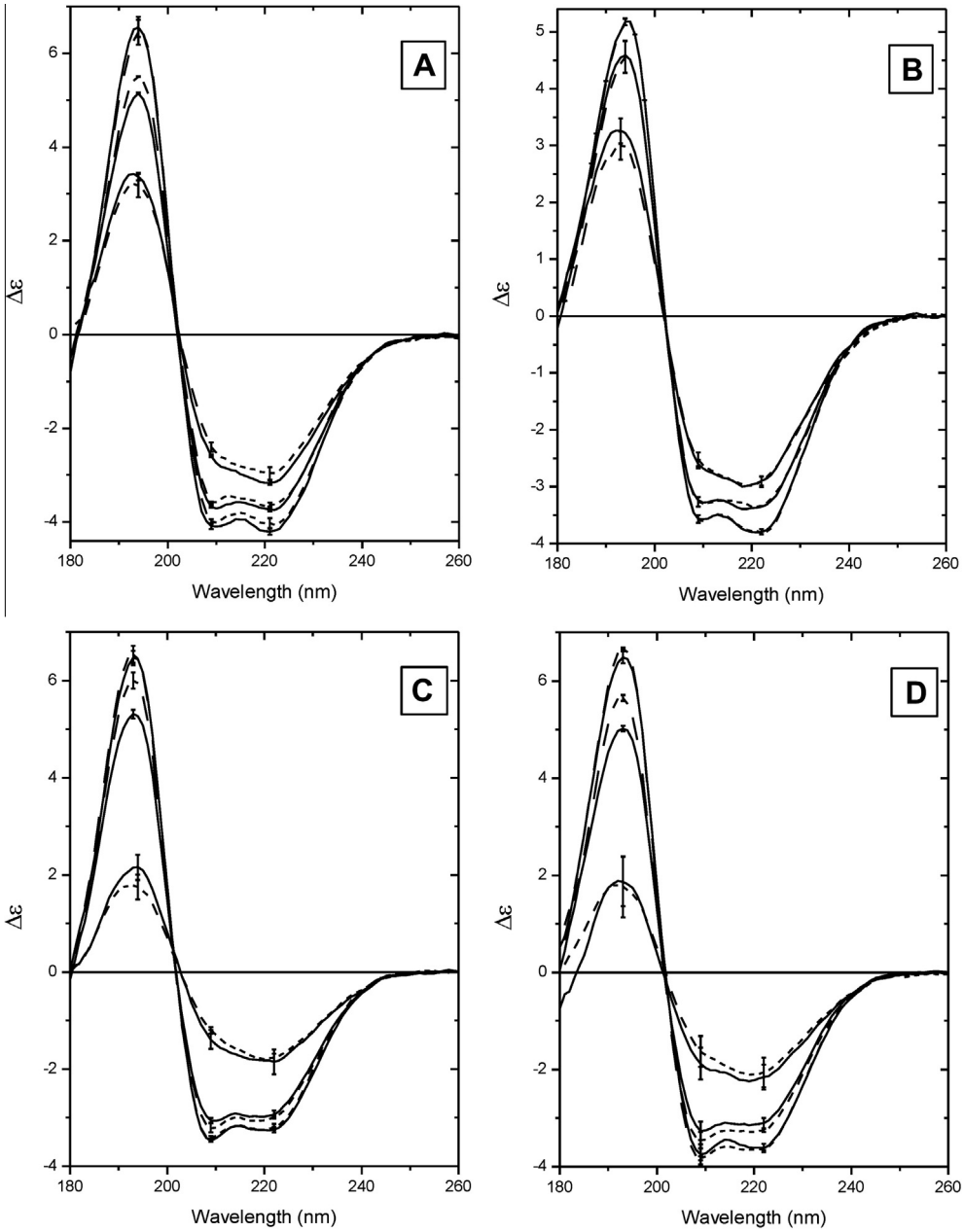

Fig. 1. Thermal denaturation of Na,K-ATPase. SRCD spectra are given for Na,K-ATPase in the absence (solid lines) and presence of 0.1 mM ouabain (dashed lines) for membranes (A, B) and for solubilised enzyme (C, D) at 20 °C and 78 °C for shark (A, C) and pig (B, D). Intermediate temperature spectra are 51 °C (A), 55 °C (B) and 37 °C for (C, D). In all panels the spectrum with the largest amplitude is that at 20 °C. In (C) the spectrum with ouabain at 37 °C is close to the 20 °C spectrum.

the E_2(K)-form [7]. For pig enzyme the midpoint of loss of Na,K-ATPase activity was 63 °C whereas it was 51 °C for shark enzyme [7]. In the present study the enzyme is predominantly in the E•Mg•Pi-form [26]. Although these two conformations have very different functional properties, we obtained the same midpoints for loss of Na,K-ATPase activity, 63 °C for pig and 51 °C for shark (data not shown) as previously observed for the E_2(K)-form [7]. In the absence of ouabain the T_m of the pig sample (61 °C, Fig. 2, filled squares) is slightly lower than the midpoint of loss of activity. For shark we find $T_m \sim 55$ °C (Fig. 2, filled circles) vs. 51 °C for loss of activity.

It is not possible to determine the temperature dependence of the loss of activity for the ouabain-bound species due to the strong inhibition of enzyme activity by ouabain.

3.3. Spectral analyses of thermaldenaturation of solubilised Na,K-ATPase

The stabilities of the enzymes were explored at different detergent/protein ratios. Thermal denaturation studies show that at a ratio of 3.3 mg/mg both enzymes show a sudden change in structure, possibly to an aggregated state (Fig. 3A and D). For the pig enzyme this occurs between 50 °C and 55 °C (Fig. 3D) whereas for the shark enzyme it occurs between 45 and 50 °C (Fig. 3A).

This behaviour is not seen when the ratio is raised to 13.3 or 26.6 mg/mg, where the denaturation curves appear smoother and the relative magnitude of change is smaller, Fig. 3B–F. As the detergent/protein ratio increases, the pig enzyme gains helix content at

Table 1
Secondary structural analyses of Na,K-ATPase samples at various temperatures.[a]

State	Temp (°C)	Ouabain	Ratio[b]	% helix	% sheet	% other
Pig enzyme						
Membrane	20	no	N/A	36 ± 2	17 ± 1	34 ± 3
Membrane	55	no	N/A	33 ± 2	19 ± 1	33 ± 1
Membrane	78	no	N/A	23 ± 1	26 ± 1	36 ± 2
			change	**−13**	**9**	**2**
Membrane	20	yes	N/A	36 ± 3	17 ± 1	34 ± 1
Membrane	55	yes	N/A	34 ± 3	21 ± 2	34 ± 2
Membrane	78	yes	N/A	23 ± 2	26 ± 2	37 ± 2
			change	**−13**	**9**	**3**
Solubilised	20	no	3.3	34 ± 2	21 ± 1	32 ± 1
Solubilised	37	no	3.3	30 ± 2	24 ± 1	33 ± 2
Solubilised	78	no	3.3	16 ± 3	31 ± 1	39 ± 1
			change	**−18**	**10**	**7**
Solubilised	20	yes	3.3	35 ± 2	20 ± 1	32 ±
Solubilised	37	yes	3.3	31 ± 2	22 ± 1	33 ± 1
Solubilised	78	yes	3.3	13 ± 5	34 ± 4	39 ± 2
			change	**−22**	**14**	**7**
Shark enzyme						
Membrane	20	no	N/A	40 ± 2	16 ± 1	33 ± 1
Membrane	51	no	N/A	34 ± 2	19 ± 1	35 ± 1
Membrane	78	no	N/A	23 ± 2	27 ± 2	36 ± 1
			change	**−17**	**11**	**3**
Membrane	20	yes	N/A	39 ± 2	16 ± 1	34 ± 4
Membrane	51	yes	N/A	35 ± 2	19 ± 1	34 ± 1
Membrane	78	yes	N/A	22 ± 3	27 ± 2	36 ± 3
			change	**−17**	**11**	**2**
Solubilised	20	no	3.3	32 ± 1	23 ± 1	32 ± 1
Solubilised	37	no	3.3	28 ± 1	26 ± 1	33 ± 1
Solubilised	78	no	3.3	13 ± 2	35 ± 2	39 ± 2
			change	**−19**	**12**	**7**
Solubilised	20	yes	3.3	31 ± 1	24 ± 1	32 ± 1
Solubilised	37	yes	3.3	29 ± 2	25 ± 2	33 ± 1
Solubilised	78	yes	3.3	10 ± 2	38 ± 2	39 ± 1
			change	**−21**	**14**	**7**

[a] Values from the algorithms CONTINLL [20,21], SELCON [22] and CDDSTR [22] (using reference set SMP180 [23]). The values reported are the average of the three algorithms, with ± reflecting the standard deviation between the values calculated by the different methods.
[b] Ratio is the detergent/protein weight ratio. "Change" refers to the difference in secondary structure % between samples at 20 and 78 °C.

Table 2
Secondary structures calculated from crystal structures.

Source	PDB ID	Ouabain	% helix[a]	% sheet	% other
Pig [4]	3KDP	no	38	11	50
Pig [5]	3N23	yes	39	14	47
Shark [3]	2ZXE	no	40	13	47
Shark [6]	3A3Y	yes	38	14	48

[a] Helix combines α-helix (H) and 3_{10} helix (G).

the expense of β-sheet but the secondary structure of shark enzyme remains the same (data not shown).

The effect of ouabain on the thermal stability of the solubilised enzymes is mixed. At the low detergent/protein ratio ouabain stabilises both shark and pig enzymes against thermal inactivation in the low-temperature regime (below 45 °C, Fig. 3A and D), as was also observed for membranous enzymes (Fig. 2). In the high-temperature regime (above 45 °C) ouabain appears to destabilise the proteins, Fig. 3A and D.

At the highest detergent/protein ratios (Fig. 3C and F) ouabain destabilises both shark and pig enzymes over the whole temperature range tested. At the intermediate detergent/protein ratio ouabain stabilises the shark enzyme against thermal denaturation at lower temperatures, whereas the pig enzyme is not stabilised by ouabain (Fig. 3B and E). At higher temperatures both shark and pig are destabilised by ouabain. For shark enzyme the temperature at which ouabain ceases to stabilise appears to be the same as the

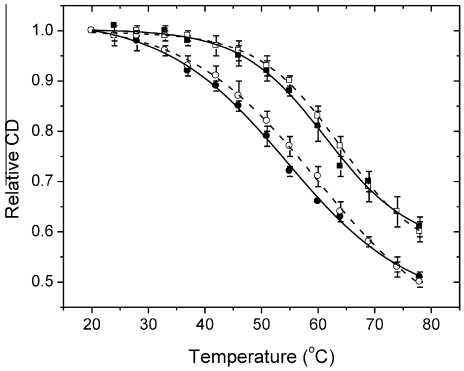

Fig. 2. Analysis of thermal denaturation. The temperature dependence of the SRCD signal was monitored at 194 nm for membrane bound shark (circles) and pig (squares) Na,K-ATPase with 0.1 mM ouabain (open symbols) and without ouabain (filled symbols). The data points were fitted with a Boltzman sigmoidal function, and the T_m values were 61.4 ± 0.9 °C for the ouabain-free and 64.0 ± 0.5 °C for the ouabain-bound pig enzyme and 54.5 ± 0.7 °C and 59.9 ± 0.9 °C for the ouabain-free and the ouabain-bound shark enzyme, respectively. The error bars represent 1 standard deviation in the measurements of three different enzyme preparations.

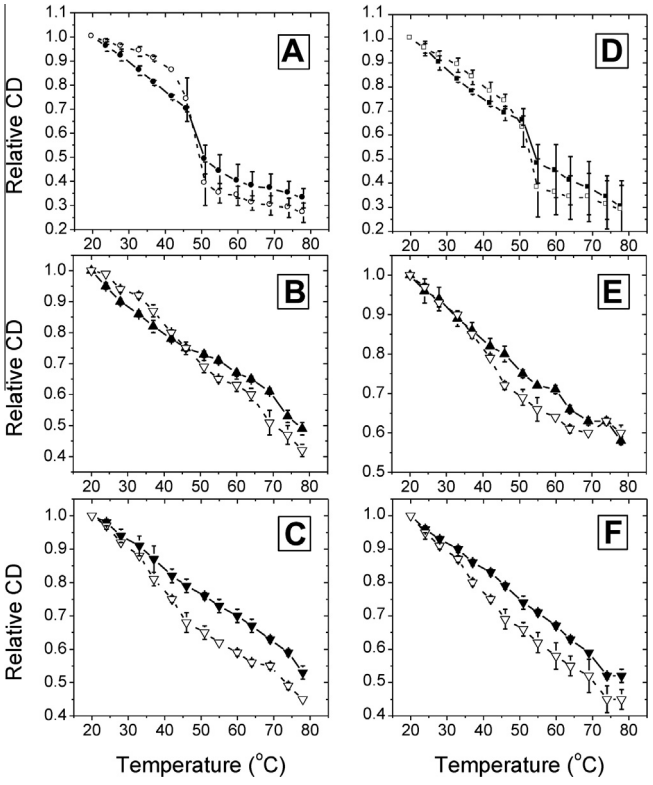

Fig. 3. Thermal denaturation curves monitored at 194 nm for solubilised Na,K-ATPase. In each panel the results are given for ouabain-free enzyme (filled symbols) and for ouabain-bound enzyme (open symbols). The error bars represent 1 standard deviation between three experiments. For shark enzyme the denaturation curves were done at detergent/protein ratios of 3.3 (A), 13.3 (B) and 26.3 mg/mg (C). Panels D, E and F show similar experiments with pig enzyme.

transition temperature at the lowest detergent/protein ratio (45–50 °C), compare Fig. 3A and B. The results presented in Fig. 3B and E, thus emphasize the transition from a native-like structure at low detergent/protein ratios (where ouabain protects, Fig. 3A and D) to the structure at high detergent/protein ratios, where ouabain has a destabilising effect on the protein structure (Fig. 3C and F).

The thermal stability of the solubilised Na,K-ATPase activity in the E•Mg•Pi-form studied here is much weaker than we previously observed for the E_2(K)-form [7]. The midpoints for loss of Na,K-ATPase activity is about 34 °C for both species at a ratio of 3.3 mg/mg. At a ratio of 13.3 mg/mg this midpoint decreases to about 26 °C for shark and less than 20 °C for pig, and at 26.6 mg/mg the midpoints are less than 20 °C for both species (data not shown). In agreement with these observations we observe ouabain-induced protections against unfolding at the low detergent/protein ratios and in the low-temperature regime, most clearly seen with the more stable shark enzyme. The loss of structure is thus preceeded by loss of enzymatic activity under these conditions.

3.4. Structural interpretation of the ouabain effect

The secondary structures as seen in the crystal structures of the pig enzyme with (PDB ID: 3N23) and without ouabain (PDB ID: 3KDP) are nearly identical (Table 2). Overlay of the structures (Fig. 4), however, reveals considerable differences in the spatial organization, and the overall impression is that the ouabain-bound form is more compact (see Ref. [5] for a detailed discussion). The major differences between the forms are the displacement of the highlighted transmembrane helix 1 of the α-subunit and the movement of its linker to the A-domain as indicated in Fig. 4 (see Ref. [5] for details).

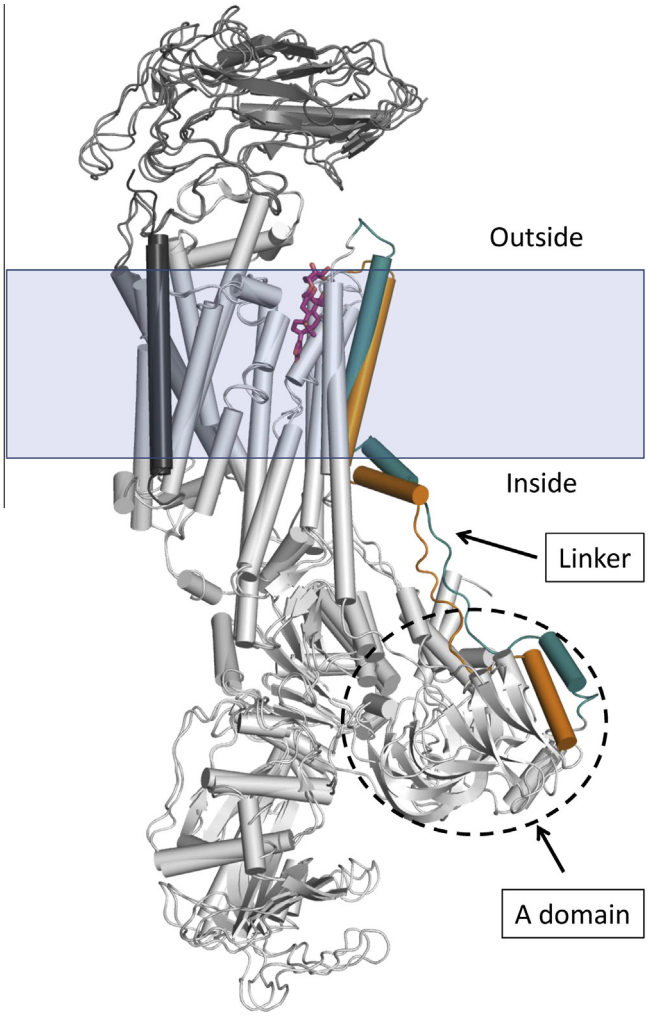

Fig. 4. Crystal structures of pig Na,K-ATPase in the presence and absence of ouabain. The α-subunit backbones are shown in grey, the ouabain molecule in pink and the location of the membrane domain in light blue. The N-terminal membrane-spanning α-helix and the linker to the A-domain is shown in green for the ouabain-free form (PDB ID: 3KDP) and in orange for the ouabain-bound form (PDB ID: 3N23). This figure was prepared using PyMOL [27]. (For interpretation of the references to colour in this figure legend, the reader is referred to the web version of this article.)

Ouabain binds in a cavity created by 6 transmembrane segments αM1–6, with its lactone ring buried within the transmembrane domain and the sugar moiety facing the extracellular side as indicated in Fig. 4. The most pronounced structural changes are observed for the transmembrane segments αM3-4: the extracellular part of αM4 undergoes a ~15° lateral tilt away from αM6, thereby providing space for ouabain binding. Hydrophobic residues Phe316 (αM4), Phe783, Phe786 (αM5) form a complementary surface to the concave surface of the steroid core and there is a hydrogen bond between hydroxyl 14 on the steroid part and Thr797 (see Ref. [5] for a detailed discussion). Thus, the access to the ion binding site from the extracellular side is hindered and the conformational rearrangements are blocked [5,6]. Upon phosphorylation of the Na,K-ATPase the transmembrane helices αM1 and αM2 undergo a conformational change which leads to movement of the αM1-2 helices towards the inhibitor molecule, extending the network of interactions between the hydrophilic surface of the steroid part of ouabain and the protein and increasing the tightness of binding [5,26]. The enzyme conformation is thus stabilised both on the extracellular side and on the intracellular side by ouabain binding, leading to higher thermal stability.

In conclusion, it is shown here using SRCD spectroscopy that Na,K-ATPase with ouabain bound is structurally more stable towards thermal denaturation than the ouabain-free form, for both the shark and pig enzymes. Since the secondary structures in general remained unaffected by ouabain binding, the increased thermal stability conferred by ouabain is most likely attributable to a reorganization of the tertiary structure. This is consistent with the crystallographic data on the pig enzyme, indicating that the protein secondary structure effectively does not change upon ouabain binding, but that the tertiary structure is altered. In detergent, the same stabilising effect of ouabain is observed at low detergent/protein ratios, where the enzyme is enzymatically active. Thus, the present study of Na,K-ATPase in solution represents added value to the information from crystal structures, as it shows that the consequence of the tertiary structure changes is a functionally-related thermal stability.

Acknowledgments

We thank Ms. Angelina Damgaard for excellent technical assistance and Mette Laursen, PhD, for providing Fig. 4. This work was supported by grants from the U.K. Biotechnology and Biological Sciences Research Council (to BAW) and beamtime grants from ASTRID (to AJM and ME). Access to the CD1 beamline at ISA is acknowledged under the EU Integrated Infrastructure Initiative (I3), European LIght Sources Activities (ELISA), under grant agreement no. 226716.

References

[1] J.H. Kaplan, Biochemistry of Na,K-ATPase, Ann. Rev. Biochem. 71 (2002) 511–535.

[2] W. Schoner, G. Scheiner-Bobis, Endogenous and exogenous cardiac glycosides: their role in hypertension, salt metabolism, and cell growth, Am. J. Physiol. Cell Physiol. 293 (2007) C509–C536.

[3] T. Shinoda, H. Ogawa, F. Cornelius, T. Toyoshima, Crystal structure of the sodium-potassium pump at 2.4 angstrom resolution, Nature 459 (2009) 446–450.

[4] J.P. Morth, B.P. Pedersen, M.S. Toustrup-Jensen, T.L.-M. Sørensen, J. Petersen, J.P. Andersen, B. Vilsen, P. Nissen, Crystal structure of the sodium-potassium pump, Nature 450 (2007) 1043–1050.

[5] L. Yatime, M. Laursen, J.P. Morth, M. Esmann, P. Nissen, N.U. Fedosova, Structural insights into the high affinity binding of cardiotonic steroids to the Na+, K+-ATPase, J. Struct. Biol. 174 (2011) 296–306.
[6] H. Ogawa, T. Shinoda, F. Cornelius, T. Toyoshima, Crystal structure of the sodium-potassium pump (Na+, K+-ATPase) with bound potassium and ouabain, Proc. Natl. Acad. Sci. (USA) 106 (2009) 13742–13747.
[7] A.J. Miles, B.A. Wallace, M. Esmann, Correlation of structural and functional thermal stability of the integral membrane protein Na, K-ATPase, Biochim. Biophys. Acta 2011 (1808) 2573–2580.
[8] M. Esmann, J.C. Skou, C. Christiansen, Solubilization and molecular weight determination of the Na, K-ATPase from rectal glands of Squalus acanthias, Biochim. Biophys. Acta 567 (1979) 410–420.
[9] J.C. Skou, M. Esmann, Preparation of membrane bound and of solubilized Na, K-ATPase from rectal glands of Squalus acanthias. The effect of preparative procedures on purity, specific and molar activity, Biochim. Biophys. Acta 567 (1979) 436–444.
[10] I. Klodos, M. Esmann, R.L. Post, Large-scale preparation of sodium-potassium ATPase from kidney outer medulla, Kidney International 62 (2002) 2097–2100.
[11] M. Esmann, ATPase and phosphatase activity of Na+, K+-ATPase: molar and specific activity, protein determination, Methods Enzymol. 156 (1988) 105–115.
[12] M. Esmann, Solubilization of Na,K-ATPase, Methods Enzymol. 156 (1988) 72–79.
[13] O.H. Lowry, N.J. Rosebrough, L. Farr, R.P. Randall, Protein measurement with the Folin phenol reagent, J. Biol. Chem. 193 (1951) 265–275.
[14] M. Esmann, J.C. Skou, Kinetic properties of C12E8-solubilized (Na^+ + K^+)-ATPase, Biochim. Biophys. Acta 787 (1984) 71–80.
[15] A.J. Miles, S.V. Hoffmann, Y. Tao, R.W. Janes, B.A. Wallace, Synchrotron Radiation Circular Dichroism (SRCD) spectroscopy: new beamlines and new applications in biology, Spectroscopy 21 (2007) 245–255.
[16] A.J. Miles, R.W. Janes, A. Brown, D.T. Clarke, J.C. Sutherland, Y. Tao, B.A. Wallace, S.V. Hoffmann, Light flux density threshold at which protein denaturation is induced by synchrotron radiation circular dichroism beamlines, J. Synchrotron. Radiat. 15 (2008) 420–422.
[17] A.J. Miles, F. Wien, J.G. Lees, A. Rodger, R.W. Janes, B.A. Wallace, Calibration and standardisation of synchrotron radiation circular dichroism and conventional circular dichroism spectrophotometers, Spectroscopy 17 (2003) 653–661.
[18] J.G. Lees, B.T. Smith, F. Wien, A.J. Miles, B.A. Wallace, CDtool - an integrated software package for circular dichroism spectroscopic data processing, analysis, and archiving, Anal. Biochem. 332 (2004) 285–289.
[19] L. Whitmore, B.A. Wallace, Protein secondary structure analyses from circular dichroism spectroscopy: methods and reference databases, Biopolymers 89 (2008) 392–400.
[20] S.W. Provencher, J. Glockner, Estimation of globular protein secondary structure from circular dichroism, Biochemistry 20 (1981) 33–37.
[21] I.H.M. Van Stokkum, H.J.W. Spoelder, M. Bloemendal, R. Van Grondelle, F.C.A. Groen, Estimation of protein secondary structure and error analysis from CD spectra, Anal. Biochem. 191 (1990) 110–118.
[22] N. Sreerama, R.W. Woody, Estimation of protein secondary structure from CD spectra: Comparison of CONTIN, SELCON and CDSSTR methods with an expanded reference set, Anal. Biochem. 287 (2000) 252–260.
[23] A. Abdul-Gader, A.J. Miles, B.A. Wallace, A reference dataset for the analysis of membrane protein secondary structures and transmembrane residues using circular dichroism, Bioinformatics 12 (2011) 1630–1636.
[24] W. Kabsch, C. Sander, Dictionary of protein secondary structure: pattern recognition of hydrogen-bonded and geometrical features, Biopolymers 22 (1983) 2577–2637.
[25] D.P. Klose, B.A. Wallace, R.W. Janes, 2-Struc: The secondary structure server, Bioinformatics 26 (2010) 2624–2625.
[26] N.U. Fedosova, F. Cornelius, I. Klodos, E2P Phosphoforms of Na, K-ATPase. I. Comparison of phosphointermediates formed from ATP and Pi by their reactivity toward hydroxylamine and vanadate, Biochemistry 37 (1998) 13634–13642.
[27] W.L. Delano, (2002) PyMOL molecular graphics system, <http://www.pymol.org>.